Available online at www.sciencedirect.com
ScienceDirect
Scripta Materialia 102 (2015) 63–66
Scripta MATERIALIA
www.elsevier.com/locate/scriptamat

Underlying structure of bulky oxide nodule on alumina-forming austenitic stainless steel

Jun-Yun Kang,[a,*] Heon-Young Ha,[a] Min-Ho Jang,[a] Joonoh Moon,[a] Dong-Woo Suh[b] and Tae-Ho Lee[a]

[a]*Korea Institute of Materials Science, 797 Changwon-daero, Changwon, Gyeongnam 642-831, Republic of Korea*
[b]*Graduate Institute of Ferrous Technology, Pohang University of Science and Technology, 77 Cheongam-ro, Nam-gu, Gyeongbuk 790-784, Republic of Korea*

Received 23 December 2014; revised 9 February 2015; accepted 10 February 2015
Available online 24 February 2015

The bulky oxide nodule and its underlying structure were investigated in an alumina-forming austenitic steel exposed to dry air at 1053 K for 336 h. Some bulky oxide nodules were found to be attached on globular phases in the matrix. By combined application of electron backscattering diffraction and energy dispersive X-ray spectroscopy, the bulky nodule was identified as Cr-rich M_3O_4 underlying which was Nb-rich MO_2. Thermodynamic calculation suggested that the MO_2 was transformed from the primary NbC near surface.

Keywords: Stainless steel; Oxidation; Electron backscattering diffraction (EBSD); Energy dispersive X-ray spectroscopy (EDXS); Phase identification

Recently, new creep- and oxidation-resistant austenitic steels which formed alumina (Al_2O_3) as protective surface oxide have been actively investigated [1–7]. These alumina-forming austenitic (AFA) steels show better oxidation resistance than the conventional chromia (Cr_2O_3)-forming alloys under wet air condition [1,6,8] as well as dry one [8], because alumina exhibits a much slower growth rate and higher thermodynamic stability than chromia [3]. The AFA steels require the addition of Al above a certain level to sustain the alumina-forming ability [1–7,9–10]. However, since Al is a strong ferrite stabilizer, excessive amounts of Al should be avoided, otherwise a considerable amount of Ni or Mn is required to obtain the stable austenitic matrix to keep the creep resistance [1–7,11–12]. Addition of Nb has been reported to play an important role in the formation of uniform external alumina film while suppressing internal oxidation [4,9–10], and also improving the creep resistance by fine NbC precipitate [1–4,11]. A number of works have been conducted to optimize the creep [1–7,11] and the oxidation resistance [1–7,9–10,13], where the creep life time and the mass change during high temperature exposure were evaluated regarding the alloy chemistry. The evolution of constituent phases in the substrate [2–5,7,11–12] and the characteristics of surface oxide [1,3,6,8–10,13] were investigated as well. However, more detailed microscopic analyses on the surface oxides are still required to understand the oxidation behavior.

In this work, we examine the characteristic features of bulky clusters of oxide nodules in an AFA steel exposed to high temperatures under dry air condition. Since such bulky clustering of oxide nodules shows the heterogeneous nature of oxide growth, understanding the formation mechanism can be contributing to control the oxidation behaviors.

The chemical composition of the AFA steel followed HTUPS 4 in [1] and is presented in Table 1. It was cast by vacuum induction melting. The cast slab of 40 mm thickness was reheated to 1523 K and held for 2 h. It was hot rolled at the temperature range between 1373 and 1173 K to the thickness of 20 mm and then quenched in water. The plate was cold rolled to the thickness of 8 mm and annealed at 1523 K for an hour followed by water quenching. Small cubic specimens were cut from the annealed plate and the surfaces were finely polished. They were then exposed to the atmospheric condition at 1053 K for 336 h.

The oxidized surfaces were observed using a field emission scanning electron microscope (JSM-7001F, JEOL). Local chemistry and crystallographic analyses were performed using electron backscattering diffraction (EBSD) and energy dispersive X-ray spectrometry (EDXS). X-Max^N EDXS detector and NordlysNano EBSD detector from Oxford instruments were used. The observation was carried out at the plane view and also at the cross sectional view. For the latter, the detailed EDXS-EBSD analysis was conducted for phase identification. For high spatial resolution in EDXS and EBSD analysis for phase identification, relatively low acceleration voltage (10 kV) and small probe

* Corresponding author. Tel.: +82 55 280 3373; fax: +82 55 280 3599; e-mail: firice@kims.re.kr

http://dx.doi.org/10.1016/j.scriptamat.2015.02.014
1359-6462/

Table 1. Chemical composition of the AFA steel (in wt.%).

C	Si	Mn	Al	Cr	Ni	Mo	Nb	B	P	Fe
0.085	0.17	2.00	2.31	14.32	20.96	2.57	0.88	0.01	0.04	Bal.

current (0.5–1 nA) were applied. For high-precision crystallographic analysis, EBSD patterns (EBSP) were recorded in the highest resolution (1344 × 1024 pixels without binning) and the maximum 12 bands were used in the indexing of EBSPs. From the compositions measured from EDXS analysis, candidate phases were carefully selected and subjected to the phase identification by EBSD. The simulated EBSPs of the candidate phases were compared with the experimental EBSP and the one which showed the best fit was finally chosen.

Plane view of the oxidized surface was repeatedly observed over a wide area where coarse oxide nodules form clusters with the dispersion of fine nodules. Figure 1 represents the typical microstructure of the oxidized surface in plane view. The elemental map of Al implies that the surface is covered by alumina as was reported elsewhere [1]. On the other hand, Al content appears to be lower in the bulky clusters, while Nb is enriched there.

Figure 2 presents a cross sectional view around the bulky nodule and corresponding chemical and crystallographic analysis results. The nodule which is exposed on the surface is sitting on a globular phase embedded in the matrix. The elemental maps for Al and Nb show that thin uniform alumina film forms at the external surface of matrix as mentioned in the plane view. It is noted that the alumina film runs through the interface which the external nodule and the globular root phase make with the matrix. The observed depletion of Al at the bulky cluster region in Figure 1 can be attributed to the formation of alumina at those interfaces instead of the outermost surface. From the Nb map in Figure 2, it is clear that the globular phase is rich in Nb. Some NbC carbide which is the brightest phase in the backscattered electron image can be also identified (marked with arrows) as reported in other previous works [2,4,11]. In Table 2, the compositions of the three marked regions in Figure 2 are presented in atomic fraction. The fraction of C is included in spite of the large uncertainty in EDXS analysis because it was not clear whether the globular root (sites 1 and 2) was carbide or not. The EBSPs from the same positions are also shown in Figure 2 overlapped with the simulated patterns of the best fitting phases. The candidate phases for EBSP indexing which were selected based on the chemistry in Table 2 are listed in Table 3. For sites 1 and 2, various carbides, oxides and intermetallic compounds as well as pure Nb are considered. All of them contain Nb basically and Fe, Cr, Al, Mn, C or O are included optionally. For site 3, as the phase is apparently a Cr-rich oxide, the oxides which contain Cr are considered with Fe, Mn or Al as minor elements. Among many Nb-containing oxides and carbides, the EBSP from region 1 showed the best match with $FeNb_2O_6$ of orthorhombic structure while that from region 2 with $FeNb_2O_6$ of tetragonal structure. Therefore, it is concluded that the globular root phase is MO_2 oxide in which M is primarily Nb while Fe, Mn, Cr or Al is also incorporated. The EBSP from region 3 showed the best match with Cr_2FeO_4 oxide of cubic structure. Thus, it is thought that the bulky oxide nodule is M_3O_4 spinel group oxide. In this case, M is primarily constituted with Cr while Fe, Mn and Al as minor elements. The detailed crystallographic information of the identified phases is presented in Table 4.

In previous studies, some Nb-rich regions were found among the surface oxides [6,10,13]. However, any detailed microscopic examination has not yet been made. On the other hand, it was revealed that the oxide nodules which formed on alumina scale were Fe, Cr or Mn-rich spinel [8,13]. Therefore, from the phase identification of site 3 in Figure 2, the bulky nodule can be considered to be excessively grown spinel nodules owing to the nonuniform progress of oxidation after the establishment of alumina film. And it is evident that the existence of Nb-rich MO_2 oxide can promote this. The formation and growth of spinel nodules are the reason for continued mass gain after the establishment of protective alumina film. Thus, it is meaningful to understand the characteristics of the nodule growth. As a part, it is required to discuss the origin of Nb-rich MO_2 beneath the bulky nodule.

The oxide phases of the given alloy were predicted from Thermo-Calc software [17] with TCFE7.0 [18] and SSUB3 [19] database. The phase equilibrium was calculated as a function of oxygen partial pressure at 1053 K and the result is shown in Figure 3. The calculation was conducted for the nominal composition given in Table 1. The minor elements, B and P were not included in the calculation as they made negligible influence on the phase equilibria due to a very small content. The calculation indicates that alumina first forms on the austenite matrix which contains NbC carbide. As oxygen partial pressure increases, other oxides such as Al_2MnO_4, chromia and Al_2SiO_5 form consuming the matrix and the preformed alumina. It is noteworthy that

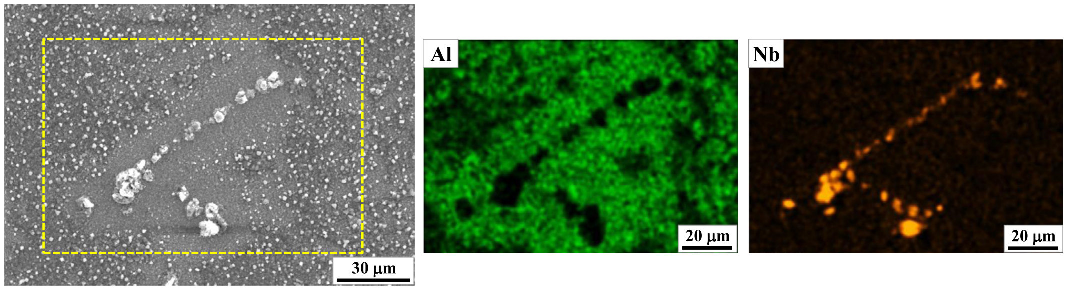

Figure 1. Secondary electron image (SEI) of oxide scale at plane view: boxed area in the SEI was subjected to EDXS mapping. The elemental maps for Al and Nb are given.